Synthesis of ZrSiN composite films using a plasma focus device

R. Ahmad[a], T. Hussain[a]†, I. A. Khan[b], and R. S. Rawat[c]

[a] Center for Advanced Studies in Physics, GC University, 54000 Lahore, Pakistan
[b] Physics Department, GC University Faisalabad, Pakistan
[c] National Institute of Education, Nanyang Technological University, Singapore 637616, Singapore

(Received 1 November 2013; revised manuscript received 3 December 2013; published online 10 April 2014)

ZrSiN thin films are synthesized by using plasma focus through various numbers of focus shots (10, 20, and 30), with samples placed at 9 cm away from the tip of the anode. Crystal structures, surface morphologies, and elemental compositions of ZrSiN films are characterized by an X-ray diffractometer (XRD) and scanning electron microscope (SEM) attached with energy dispersive X-ray spectroscopy (EDS). XRD patterns confirm the formations of polycrystalline ZrSiN films. Crystallinity of nitride increases with the increase of focus shot number. The average crystallite size of zirconium nitride increases from 27 ± 3 nm to 73 ± 8 nm and microstrain decreases from 2.28 to 1.0 with the increase of the focus shot number. SEM results exhibit the formations of granular and oval-shaped microstructures, depending on the number of focus shots. EDS results confirm the presences of silicon, zirconium, nitrogen, and oxygen in the composite films. The content values of Zr and N in the composite films increase with the increase of the focus shot number.

Keywords: DPF, ZrSiN thin films, XRD, SEM

PACS: 52.59.Hq, 52.77.Dq, 61.05.cp, 68.37.Hk **DOI:** 10.1088/1674-1056/23/6/065204

1. Introduction

Transition metal nitrides such as ZrN, TiN, and HfN have extensively been studied as hard coatings[1] on cutting tools and molding dies. Addition of the third element like Al, Cu, and Si into these compounds has shown significant improvement in mechanical properties and oxidation resistance.[2,3] Intensive efforts have been made to synthesize composite films like TiAlN, TiSiN, TiAlZrN, TiAlSiN, TiBN, and TiCN[4,5] to enhance the chemical and mechanical properties of these films. Comparatively, TiSiN is more attractive because of its high hardness and better stability.[4,5] However, there are few investigations on the ternary metal nitride composite films like ZrSiN.[3,6–9] It has been shown that the addition of Si into ZrN results in the refinement of the grains of the composite structure. Such ternary metal nitride composite films have been deposited using different deposition techniques like DC magnetron sputtering,[9] RF reactive sputtering,[8] and chemical vapor deposition.[10] However, a high temperature environment and longer deposition times are required to deposit the composite films as reported in Refs. [11] and [12]. Plasma focus (PF) is a simple device which is being used to deposit composite films on different substrates at ambient temperature.

The plasma focus device is a coaxial plasma accelerator capable of producing dense (10^{25} m^{-3}–10^{26} m^{-3}) and hot (1 keV–2 keV) plasma of short time duration ($\approx 10^{-7}$ s).[13] It is a rich source of hard and soft X-rays, neutrons, highly energetic ions, and relativistic electrons over a broad energy spectrum.[14] Ion beams emitted from PF devices have been effectively employed in plasma-assisted surface modification including thermal surface treatment, ion implantation, phase changes in thin films, and thin films deposition.[15–18] The relativistic electrons are also used to ablate the material (placed at the anode tip) which reacts with the nitrogen plasma and to sputter the substrate material to form composite films. Films deposited by this device show superior surface qualities including good adhesion to the substrate surface and grain growth of different compounds through nucleation by successive focus shots at ambient temperature[19] and short nitriding time duration.

Our plasma research group have already grown TiN/Si_3N_4, nc-(Ti, Al) N/a-Si_3N_4, and TiN/Ni_3N/a-Si_3N_4 thin composite films using the dense plasma focus device.[20–22] In the present work, we synthesize composite (ZrSiN) films on silicon substrates at ambient temperature using the PF device. Microstructures, crystallite sizes, microstrains, texture coefficients, surface morphologies, and elemental concentrations of the composite films are investigated in terms of focus shots.

2. Experimental details

Deposition of composite (ZrSiN) films is accomplished by using a PF device which is powered by a single Maxwell 32 μF, 15 kV, fast discharging capacitor bank with a maximum storage energy of 3.3 kJ. The details of the PF facility are given elsewhere.[16,23] The focus machine with an engraved copper anode is optimized for strong focusing at different nitrogen filling gas pressures. An optimal pressure of 1.25 mbar (1 bar = 10^5 Pa) is used for the present experiment whereas

*Project supported by the National Project for Research for University, the Higher Education Commission (HEC), Pakistan.
†Corresponding author. E-mail: tousifhussain@gcu.edu.pk
© 2014 Chinese Physical Society and IOP Publishing Ltd

the charging voltage of the machine is kept at 12 kV. The high voltage probe, Rogowski coil and photodiode signals are monitored by a digital oscilloscope connected to a computer.

A BPX65 photodiode detector placed at 9 cm in front of the central anode is employed to characterize the nitrogen ions emanated during the radial collapse phase of the PF device. The details of the BPX65 photodiode detector is described elsewhere.[15] A typical ion beam signal recorded by the photodiode and a high voltage probe signal are used for estimating the different ion beam parameters such as ion energy (E), ion number density (N_d), and total number of ions reaching the substrate surface (Fig. 1). These characteristic nitrogen ions are then utilized for the deposition of composite (ZrSiN) films, and the relativistic electrons coming out from the focus also ablate the inserted material (zirconium) placed at the anode tip. Silicon samples placed at 9 cm away from the central anode, located at 0° angular positions with respect to the anode axis are exposed to multiple (10, 20, and 30) focus shots.

Crystal structures, surface morphologies, and elemental compositions of the deposited composite (ZrSiN) films are examined by employing an X-ray diffractometer (XRD), scanning electron microscope (SEM) attached with energy dispersive X-ray (EDX) spectroscopy. The analyses of crystallite sizes and microstrains are also performed by using the Williamson–Hall (WH) method from the X-ray diffraction data.

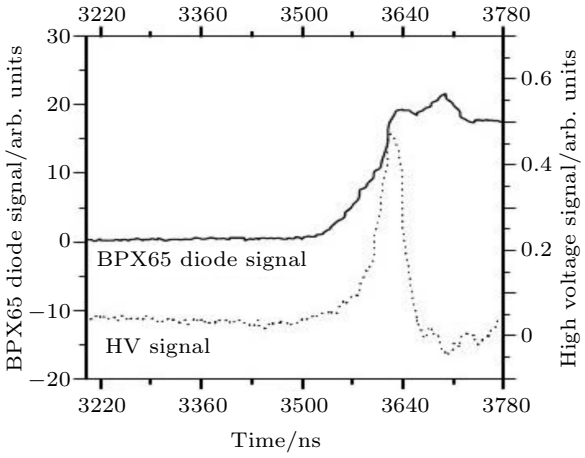


Fig. 1. A typical ion beam signal recorded by the BPX65 photodiode detector along with the high voltage probe signal, placed at 9 cm along the anode axis.

3. Results and discussion

Ion beam signals (solid line) recorded with the photodiode detector placed at 9-cm axial position and the high voltage signal (dotted line) are shown in Fig. 1. The first peak in the diode signal represents the X-ray pulse while the second peak indicates the desired ion beam pulse. Such ion beam pulses have already been reported in the literature.[24] Ion beam signals are averaged over ten signals to estimate the average values of the ion beam parameters like ion energies and ion number densities for different focus shots. It is found that ion energies range from 45 keV to 480 keV while their corresponding ion number densities are in the range from 9.39×10^{16} cm^{-3} to 2.9×10^{16} cm^{-3}. It is known that ions are emitted in a fountain-like geometry with angular anisotropy. Most of the ions are emitted in a small solid angle along the anode axis and their fluxes decrease with increasing angle.[25] A total number of nitrogen ions reaching the substrate surface during one focus shot of duration ~ 80 ns is 5.23×10^{12} as shown in Fig. 1. These results are consistent with those in the literature.[15] In the deposition process, these energetic nitrogen ions deliver enough energy to the substrate surface, thereby raising the substrate surface transient temperature, which results in local melting and evaporation. Eventually, the original phase of silicon re-crystallizes with the development of new phases in the molten state.[26]

3.1. Phase identification

XRD patterns of the composite ZrSiN films deposited for multiple (10, 20, and 30) focus shots when the samples are placed at 9 cm away from the tip of the anode along the anode axis are shown in Fig. 2. For 10 focus shots, various diffraction peaks related to silicon/zirconium nitrides [01-071-0623, 00-005-0659, 00-041-0360, 01-076-0503, 01-075-0950, and 01-087-0842] are evolved. This confirms the formations of polycrystalline composite (ZrSiN) films. The diffraction peaks are also broadened, indicating the formations of nano-crystallites as the crystallite size is inversely related to the peak broadening. This shows that 10 focus shots are sufficient for the nucleation of nitrides as well as for the re-crystallization of silicon.

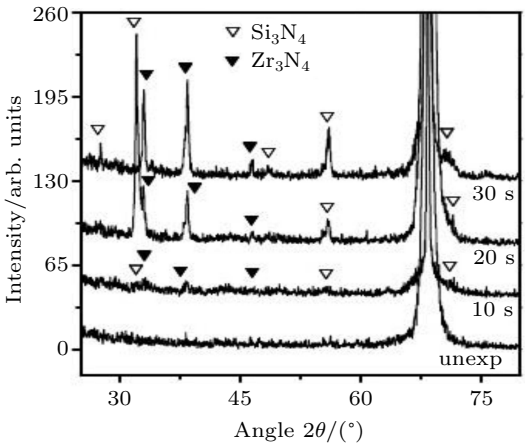


Fig. 2. XRD patterns of the composite (ZrSiN) films deposited for multiple (10, 20, and 30) focus shots at 0° angular position.

For 20 focus shots, the crystallinities of silicon/zirconium nitride phases increase. For 30 focus shots, the crystallinities of all these phases increase except the crystallinity of the (130) phase of silicon nitride, which disappears. Moreover, the XRD patterns clearly show that there is no oxide peak. This indicates that native oxides may be removed from the sample surface exposed at 0° angular position. Table 1 shows the

occurrences of diffraction peaks of silicon/zirconium nitrides along with their 2θ and hkl values. The diffraction peaks appearing for 10 focus shots are slightly shifted from their standard database values. No further shift in the diffraction peaks is observed with the increase of the focus shot number (20 and 30 shots). At 0° angular position, energetic ions are used not only to deposit the materials but also to sputter the substrate or already deposited film.

Table 1. Various diffraction peaks of silicon/zirconium nitrides appearing at various 2θ values observed from the XRD patterns.

Number of focus shots	Sample angular positions	Various diffraction peaks of silicon/zirconium nitrides observed at various 2θ positions			
		Si_3N_4		Zr_3N_4	
		2θ	hkl	2θ	hkl
10	0°	31.94	1 3 0	32.98	2 0 1
		55.91	4 0 0	38.27	1 3 1
		71.48	8 4 0	46.44	401
20	0°	31.94	1 3 0	32.98	2 0 1
		55.91	4 0 0	38.27	1 3 1
		71.48	8 4 0	46.44	4 0 1
30	0°	27.3	2 0 0	32.98	2 0 1
		48.42	0 4 2	38.27	1 3 1
		55.91	4 0 0	46.44	4 0 1
		71.48	8 4 0		

Moreover, the disappearance of the (130) phase of silicon nitride for 30 focus shots may be due to its re-sputtering and evolution of the new silicon nitride phase. Thus, this phase of silicon nitride is not stable for a higher number of focus shots.

The broadened peaks indicate the formations of nano-crystallites and the presences of microstrains in the composite films. These microstrains are attributed to the lattice distortions and imperfections developed in the composite films.

The broadening due to crystalline imperfections can be separated into two parts according to the Williamson–Hall (WH) method[27] which is given as follows:

$$B_{\rm r} = \frac{k\lambda}{L\cos\theta} + \eta\tan\theta.$$

In the above equation, the first term on the right-hand side indicates the broadening due to nano-crystallites whereas the second term shows the broadening due to lattice strain. Figure 3(a) shows a WH plot (between $B_r\cos\theta$ and $\sin\theta$) for the composite (ZrSiN) films deposited for 30 focus shots when the sample is placed along the anode axis. This gives a straight line having slope η and intercept $(k\lambda/L)$ where λ is the wavelength, k is a numerical constant ($k = 0.94$), and L is the crystallite size. The crystallite size L and microstrains developed in the composite films can be determined from the intercept and slope respectively.

The average crystallite size of the Zr_3N_4 phase increases with the increase of the focus shot number (Fig. 3(b)). It varies from 27 ± 3 nm (for 10 shots) to 73 ± 8 nm (for 30 shots). On the other hand, the average microstrain value decreases with the increase of focus shot number. The maximum microstrain value of the film deposited for 10 focus shots is found to be 2.28 and decreases to 1.0 (30 focus shots) with the increase of the focus shot number.

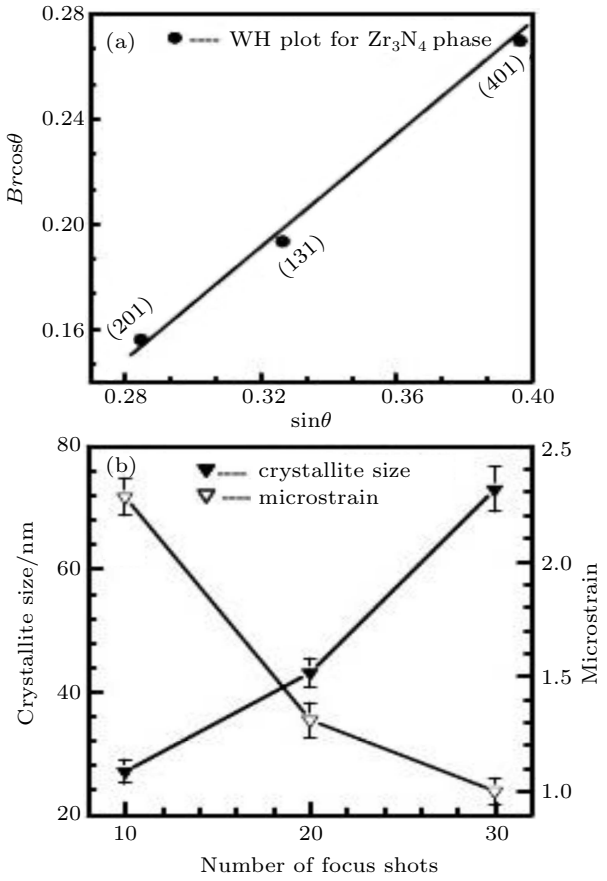


Fig. 3. (a) Williamson–Hall plot for the composite film deposited for 30 focus shots at 0° angular position and (b) average crystallite size and microstrain measurements versus focus shot number.

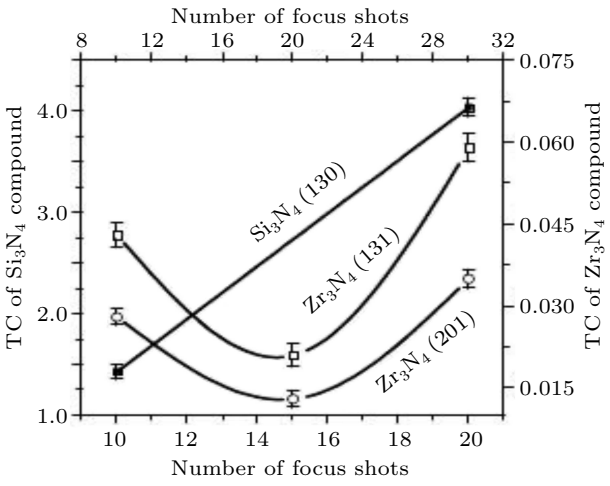


Fig. 4. Texture coefficients of Si_3N_4 (130) and Zr_3N_4 (102) and (131) planes each as a function of focus shot.

Maximum microstrains developed in the composite films could probably be due to the re-crystallizations of silicon and nucleations of nitride phases. The reduction in microstrain shows a stress relaxation in the composite film. This

stress relaxation is attributed to the rise in surface transient temperature followed by successive focus shots, which result in the enhanced crystalinities of nitrides. This improvement in the crystal growth of nitride reduces the microstrains and defects because defects are directly related to the crystallite size. The bigger crystallite size minimizes the grain boundary area, which reduces the diffusion as well as the electromigration,[28] resulting in stress relaxation.

The preferred orientation of various diffraction planes is determined by estimating the texture coefficient $TC_{(hkl)}$ from the following expression:[29]

$$TC_{(hkl)} = \frac{I_{(hkl)}/I_{0(hkl)}}{N^{-1}\sum I_{(hkl)}/I_{0(hkl)}},$$

where I and I_0 are the measured and standard intensities respectively, and N is the number of reflections planes.

Figure 4 exhibits the texture coefficients of Zr_3N_4 (131), (102), and Si_3N_4 (130) planes, each as a function of the focus shot number. The texture coefficients of Zr_3N_4 (131) and (201) planes first decrease from 0.043 to 0.021 (10 to 20 focus shots) and then increases to 0.059 for 30 focus shots. However, similar trends in the texture coefficients of both Zr_3N_4 (131) and (201) planes are observed. On the other hand, the texture coefficient of Si_3N_4 (130) plane is 1.43 for 10 focus shots and it increases to 4.1 for 20 focus shots. However, the decreases in texture coefficients of Zr_3N_4 (131) and (201) planes (for 20 shots) may be due to the abrupt increase in the texture coefficient of Si_3N_4 (130) plane. This increase in the texture coefficient of Si_3N_4 (130) plane may be due to the increase in its crystallinity. Its crystallinity may be increased due to enhanced adatom mobility, which reduces its surface energy. Thus a lower surface energy may enhance the texture coefficient of silicon nitride along the (130) orientation. However, the rapid increase in the texture coefficient of Si_3N_4 (130) plane changes its preferred orientation. It means that the (130) plane of silicon nitride disappears while the crystallinity of the zirconium nitride plane increases for 30 focus shots.

3.2. Surface morphology

Figure 5 exhibits the surface morphologies of the composite films deposited at 0° angular position for multiple (10, 20, and 30) focus shots. At 0° angular position (10 focus shots), a uniform composite film showing rounded grains is

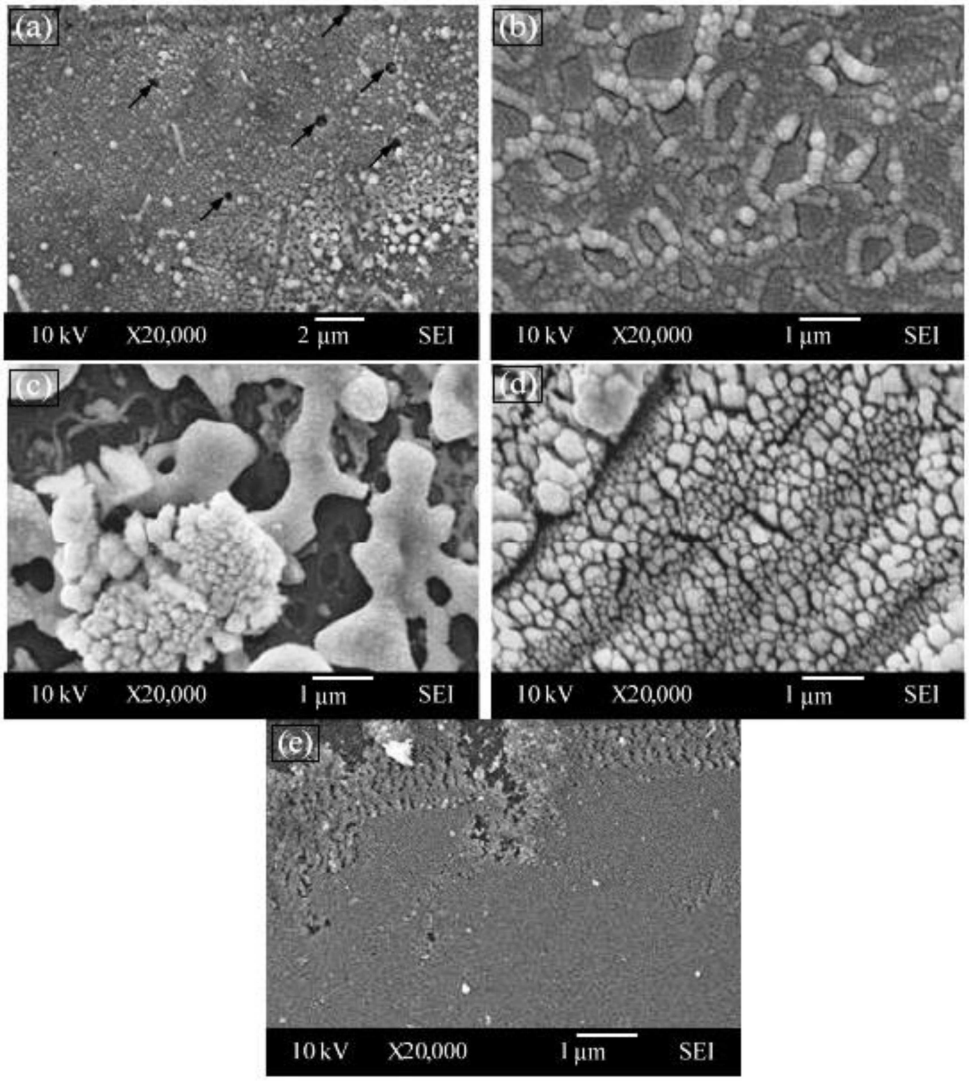


Fig. 5. SEM microstructure patterns of the composite films deposited for multiple (10, 20, and 30) focus shots, (a), (b), and (c) at 0° angular positions.

formed (Fig. 5(a)). However, few pores of ~ 400 nm in size are also observed. For 20 focus shots, the grain sizes of nitrides increase, accompanied with the appearance of an oval shape surface (Fig. 5(b)). This oval shape surface is free of nano-pores. This may be due to the grain growths and crystallinities of nitrides, which is attributed to the rise in surface transient temperature followed by successive focus shots. However, the composite film is not smooth. This may be due to the formations of grains of different sizes. Moreover, a coagulation of grains is also observed. This type of grain growth and their coagulations in the plasma focus ion-assisted films have already been reported.[30] The formations of clusters consisting of nano-grains (80 ± 5 nm) (Figure. 5(c)) is attributed to the increase of focus shot number (30 shots). The melting and swelling (Fig. 5(c)) of the surface are also observed, which may be due to more energy deliverance to the substrate during ion bombardment. Thus, a rough surface is obtained due to melting, swelling, and cluster formation. The re-sputtering of the silicon nitride (130) phase may be the other reason. It is concluded that microstructure patterns of the composite films depend on the number of focus shots and the rise in the surface transient temperature of the substrate during the deposition process.

Figure 6 shows a relationship between the elemental concentration and the focus shot number. The silicon content value decreases while zirconium and nitrogen content values increase in the composite film deposited up to 20 focus shots (Fig. 6). For 30 focus shots, the silicon content value increases slightly while the nitrogen content value decreases in the composite film. This decrease in the nitrogen content value may be due to the re-sputtering of silicon nitride. EDX data show that the composite films deposited along the anode axis are free of oxides. These results accord well with the XRD results since there is no oxide peak and therefore only nitride peaks of silicon/zirconium occurs there. This confirms the complete nitridation of silicon substrate along the anode axis.

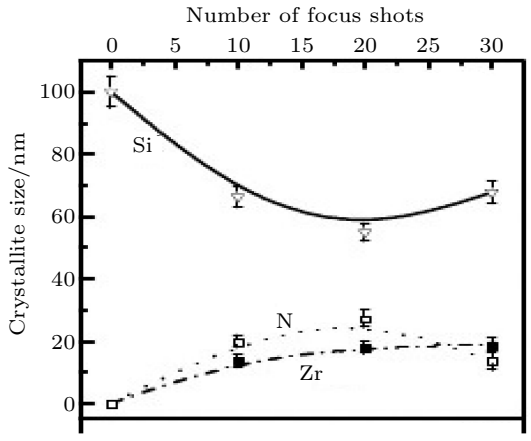


Fig. 6. EDX data showing the presences of silicon, zirconium, nitrogen, and oxygen in the composite films deposited for multiple (10, 20, and 30) focus shots at 0° angular positions.

4. Conclusions

The plasma focus device is used to deposit composite (ZrSiN) films on silicon substrates at ambient temperature. Composite (ZrSiN) films are deposited for multiple (10, 20, and 30) focus shots and at 0° angular positions. The ion energy ranges from 45 keV to 480 keV and relativistic electron beams are used for depositing the composite (ZrSiN) films. XRD patterns confirm the depositions of polycrystalline composite films. The crystallinities of silicon/zirconium nitrides increase with the increase of the focus shot number. The average crystallite size of zirconium nitride increases from 27 ± 3 nm to 73 ± 8 nm while microstrain values for the composite films decrease from 2.28 to 1.0 with the increase of the focus shot number, resulting in the enhanced crystallinities of nitrides. Texture coefficient of Si_3N_4 (130) plane is found to be 4.1 for the composite film deposited for 20 focus shots. SEM results show that a smooth film showing granular surface morphology is observed for 10 focus shots. An oval shape microstructure (free from nano-pores) with compact film appearance is observed for 20 focus shots. Clusters are formed in the composite film deposited for 30 focus shots along with the melting and swelling of the substrate surface. EDX data confirm the presence of silicon, zirconium, nitrogen, and oxygen in the deposited composite films.

References

[1] Oberländer B C, Franck M, Campbell P, Celis J P, Roos J, Hellemans L and Snauwaert J 1994 *Thin Solid Films* **241** 222
[2] Vaz F, Rebouta L, Ramos S, da Silva M F and Soares J C 1998 *Surface and Coatings Technology* **108–109** 236
[3] Pilloud D, Pierson J F, Marco de Lucas M C and Alnot M 2004 *Appl. Surf. Sci.* **229** 132
[4] Heim D and Hochreiter R 1998 *Surface and Coatings Technology* **98** 1553
[5] Holubář P, Jílek M and Šíma M 1999 *Surface and Coatings Technology* **120–121** 184
[6] Brandstetter E, Mitterer C and Ebner R 1991 *Thin Solid Films* **201** 123
[7] Mae T, Nose M, Zhou M, Nagae T and Shimamura K 2001 *Surface and Coatings Technology* **142–144** 954
[8] Nose M, Zhou M, Nagae T, Mae T, Yokota M and Saji S 2000 *Surface and Coatings Technology* **132** 163
[9] Pilloud D, Pierson J F, Marques A P and Cavaleiro A 2004 *Surface and Coatings Technology* **180–181** 352
[10] Winkelmann A, Cairney J M, Hoffman M J, Martin P J and Bendavid A 2006 *Surface and Coatings Technology* **200** 4213
[11] Rie K T and Wöhle J 1999 *Surface and Coatings Technology* **112** 226
[12] Hollstein F, Kitta D, Louda P, Pacal F and Meinhardt J 2001 *Surface and Coatings Technology* **142–144** 1063
[13] Lee S, Tou T Y, Moo S P, Eissa M A, Gholap A V, Kwek K H, Mulyodrono S, Smith A J, Suryadi, Usada W and Zakaullah M 1988 *Am. J. Phys.* **56** 62
[14] Takao K, Honda T, Kitamura I and Masugata K 2003 *Plasma Sources Science and Technology* **12** 407
[15] Mohanty S R, Neog N K, Nayak B B, Acharya B S, Lee P, Tan T L and Rawat R S 2006 *Nucl. Instrum. Methods Phys. Res. Sec. B: Beam Interactions with Materials and Atoms* **243** 113
[16] Rawat R S, Lee P, White T, Ying L and Lee S 2001 *Surface and Coatings Technology* **138** 159
[17] Rawat R S, Aggarwal V, Hassan M, Lee P, Springham S V, Tan T L and Lee S 2008 *Appl. Surf. Sci.* **255** 2932

[18] Hussain T, Ahmad R, Khalid N, Umar Z and Hussnain A 2011 *Nucl. Instrum. Methods Phys. Res. Sec. B: Beam Interactions with Materials and Atoms* **269** 1951
[19] Hussain T, Ahmad R, Khalid N, Umar Z and Hussnain A 2013 *Chin. Phys. B* **22** 055204
[20] Umar Z A, Ahmad R, Khan I A, Hussain T, Hussnain A, Khalid N, Awais A and Ali T 2013 *Radiation Effects and Defects in Solids* **168** 892
[21] Ahmad R, Hassan M, Murtaza G, Akhter J I, Qayyum A, Waheed A and Zakaullah M 2006 *Radiation Effects and Defects in Solids* **161** 121
[22] Kelly H, Lepone A, Marquez A, Sadowski M J, Baranowski J and Skladnik-Sadowska E 1998 *IEEE Trans. Plasma Sci.* **26** 113
[23] Bertalot L, Herold H, Jäger U, Mozer A, Oppenländer T, Sadowski M and Schmidt H 1980 *Phys. Lett. A* **79** 389
[24] Feugeas J N, Sanchez G, De Gonzalez C O, Hermida J D and Scordia G 1994 *Radiation Effects and Defects in Solids* **128** 267
[25] Williamson G K and Hall W H 1953 *Acta Metallurgica* **1** 22
[26] Bhuvaneswari H B, Rajagopal Reddy V, Chandramani R and Mohan Rao G 2004 *Appl. Surf. Sci.* **230** 88
[27] Rawat R S, Aggarwal V, Hassan M, Lee P, Springham S V, Tan T L and Lee S 2008 *Appl. Surf. Sci.* **255** 2932
[28] Akyuz I, Kose S, Atay F and Bilgin V 2006 *Semicond. Sci. Technol.* **21** 1620
[29] Hussain T, Ahmad R, Khan I, Siddiqui J, Khalid N, Bhatti A S and Naseem S 2009 *Nucl. Instrum. Methods Phys. Res. Sec. B: Beam Interactions with Materials and Atoms* **267** 768
[30] Hassan M, Qayyum A, Ahmad R, Murtaza G and Zakaullah M 2007 *J. Phys. D: Appl. Phys.* **40** 769